



Science and Engineering Symposium
4th International Science, Social Science, Engineering and Energy Conference 2012

Theoretical calculations of electronic structure and thermoelectric properties of CuGaO₂

P. Poopanya^{a,*}, R. Nakowong^a, A. Yangthaisong^b, T. Seetawan^c

^aProgram of Physics, Faculty of Science, Ubon Ratchathani Rajabhat University, Ubon Ratchathani, 34000, Thailand

^bComputational Materials and Device Physics Group, Department of Physics, Faculty of Science, Ubon Ratchathani University, Ubon Ratchathani 34190, Thailand

^cThermoelectrics Research Center and Program of Physics, Faculty of Science and Technology, Sakon Nakhon Rajabhat University, Sakon Nakhon 47000, Thailand

Abstract

The thermoelectric properties of delafossite material CuGaO₂ have been investigated by theoretical calculations. The energy band structures were calculated using the total energy plane-wave pseudopotential method. The calculated equilibrium lattice parameters $a = 2.944 \text{ \AA}$ and $c = 16.933 \text{ \AA}$ are in good agreement with both the experimental and theoretical data. CuGaO₂ has shown an indirect band gap material around 1.101 eV. The calculated energy band structures are used in combination with the Boltzmann transport equation solver to calculate the electrical conductivity (σ) and Seebeck coefficient (S) under the constant scattering time (τ) approximation. The scattering time of approximately $0.4 \times 10^{-16} \text{ s}$ is obtained, fitting the calculated Seebeck coefficient and electrical conductivity with the recent measurement. By considering the effect of the doping level and temperature, it is found that the Seebeck coefficient increases with increasing acceptor doping level and decreases with increasing temperature, while the electrical conductivity increases as the temperature and doping level increase. This leads to the large power factor ($S^2\sigma$) for a low acceptor doping level and high temperature. The calculated power factor shows the maximum carrier density of hole at around $1 \times 10^{21} \text{ cm}^{-3}$ to $5 \times 10^{21} \text{ cm}^{-3}$. Additionally, our study suggests that CuGaO₂ can be considered as a promising thermoelectric material at high temperature.

© 2013 The Authors. Published by Kasem Bundit University.

Selection and/or peer-review under responsibility of Faculty of Science and Technology, Kasem Bundit University, Bangkok.

Keywords: Thermoelectric properties; Electronic structure; CuGaO₂; Constant scattering time; Acceptor doping level

1. Introduction

Thermoelectric (TE) materials and devices have been attracted an intense interest because of their potential applications as energy conversion, sensors, and TE coolings. The efficiency of TE performance could be defined by figure of merit, $Z = S^2\sigma/\kappa$ [1]. Note S , σ and κ are the Seebeck coefficient, electrical conductivity, and

* Corresponding author. E-mail address: lookdok@hotmail.com

thermal conductivity, respectively. The high performance TE materials require high power factor ($PF = S^2\sigma$) and low thermal conductivity. However, it is very difficult to control these parameters independently since the Seebeck coefficient is inversely related to the electrical conductivity. Besides, the reduction of the thermal conductivity leads to the decrease of the electrical conductivity. Hence, the investigation on TE materials relies on increasing electronic transport properties and decreasing thermal conductivity [2, 3].

Recently, it was reported that the delafossite structure material is one of high potential TE materials [4]. The delafossite structures have the formula $A^{II}B^{VI}O^{IV}_2$, where the *A* site is host to a monovalent cation (Cu, Ag, Pd, and Pt), the *B* site is host to a trivalent transition metal cation (Al, Co, Cr, Ga, In, Y, etc) [5]. Their crystalline structures belong to the space group R-3m, which can be viewed as an alternative stacking of the *A* and BO_2 layers perpendicular to the *c*-axis as shown in Fig. 1(a). The $CuBO_2$ materials have been attracted attention due to their layered structure with hexagonal symmetry and the different sizes of the *B* atom, leading to different values of the electrical conductivity. Therefore, $CuBO_2$ has been widely studied experimentally [6-8] and theoretically [9-11] in order to improve the electrical conductivity or TE properties. We have successfully performed the calculations of the electronic structures and TE properties of doped $CuAlO_2$ material [12] using the same method as in this paper. Technically, the electronic structures of delafossite $CuGaO_2$ were calculated using first principles calculations. The calculated band structures are then used in combination with the Boltzmann transport equation (BTE) solver under the constant scattering time approximation [13] to calculate the TE properties of $CuGaO_2$. Note that the rigid band approach is employed in our calculations [14, 15].

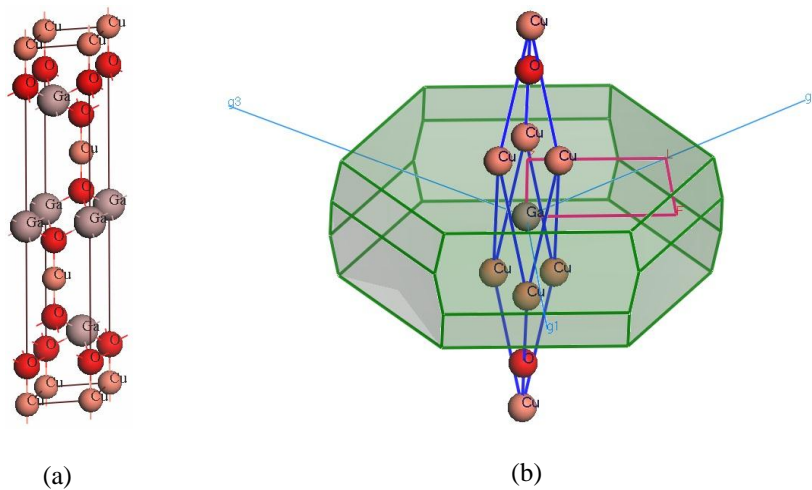


Fig. 1. Crystal structure of delafossite $CuGaO_2$: (a) conventional unit cell; (b) primitive cell in reciprocal space with first Brillouin zone and high symmetry points

This paper is organised as follows: we briefly describe the technical details used in this work in Computational Details. The structural, electronic and TE properties are presented in Results and Discussion. Finally, the results of our calculation are summarized in Conclusion.

2. Computational Details

The space group of delafossite $CuGaO_2$ is R-3m. The corresponding Wyckoff positions are Cu (0,0,0), Ga (0,0,0.5) and O (0,0,z) [16]. The energy band structures were calculated using the pseudopotential method as implemented in CASTEP code [17] which was based on density functional theory (DFT). The states $Cu-3p^6 3d^{10}4s^1$, $Ga-3d^{10}4s^24p^1$ and $O-2s^22p^4$ were taken as valence electrons. The presence of tightly bound core electrons was represented by ultrasoft Vanderbilt-type pseudopotentials. The exchange-correlation potential was

treated within local-density approximation (LDA). A plane-wave cutoff energy of 380 eV was used throughout the calculation. Geometry optimization was achieved using convergence thresholds of 5×10^{-6} eV/atom for total energy, 0.01 eV/Å for maximum force, 0.02 GPa for pressure and 0.0005 Å for displacement. The tolerance in the self-consistent field (SCF) calculation is 5×10^{-7} eV/atom. The Monkhorst-Pack \bar{k} point set is $30 \times 30 \times 30$ which has approximately 2,250 \bar{k} point in the irreducible part of the Brillouin zone. The calculated energy band structures were then used in combination with the BoltzTraP program [18] to calculate the TE properties of CuGaO₂.

The constant scattering time approximation was used in the BTE to calculate the electrical transport coefficient, especially in the calculation of the Seebeck coefficient and electrical conductivity. In this approximation, it was assumed that the scattering time is an energy-independent parameter and does not depend on temperature and doping level, so that the scattering time can be cancelled in the expression for the Seebeck coefficient tensor. Thus, the Seebeck coefficient tensor can be expressed as:

$$S_{\alpha\beta} = \sum_{\gamma} (\sigma^{-1})_{\alpha\gamma} v_{\alpha\beta}, \quad (1)$$

where $v_{\alpha}(i, \bar{k})$ are the component of the band velocity. Note that the band velocity can be calculated from

$$v_{\alpha\beta}(T, E_F) = \frac{1}{eT\Omega} \int \sigma_{\alpha\beta}(\varepsilon)(\varepsilon - E_F) \left[-\frac{\partial f_{E_F}(T, \varepsilon)}{\partial \varepsilon} \right] d\varepsilon \quad (2)$$

where f_{E_F} is the Fermi distribution function, E_F is the Fermi energy, e is the electron charge, T is temperature and Ω is the volume. The conductivity tensor $\sigma_{\alpha\beta}$ is given by

$$\sigma_{\alpha\beta}(i, \bar{k}) = e^2 \tau_{i, \bar{k}} v_{\alpha}(i, \bar{k}) v_{\beta}(i, \bar{k}) \quad (3)$$

In order to calculate the transport distribution in Eq. (1)-(3), the group velocity, the energy, and the scattering time are needed for each \bar{k} point. A direct calculation of the group velocity, using the definition, is given by

$$\bar{v}_i(\bar{k}) = \frac{\nabla_{\bar{k}} \varepsilon_i(\bar{k})}{\hbar} \quad (4)$$

Note that the group velocity in Eq. (4), is a gradient in reciprocal space of the dispersion relation or band structure of the electrons in crystal or material.

3. Results and Discussion

The calculated lattice constants of the conventional cell delafossite CuGaO₂ are $a = 2.944$ Å and $c = 16.933$ Å. These values are in good agreement with the experimental data: $a = 2.976$ Å, $c = 17.160$ Å [19], $a = 2.857$ Å, $c = 16.940$ Å [20], $a = 3.005$ Å, $c = 17.122$ Å [21] and the theoretical data: $a = 2.955$ Å, $c = 17.015$ Å [22], $a = 2.977$ Å, $c = 17.171$ Å [23]. Figure 2 shows the calculated energy band structure and partial density of states (PDOS). The energy band structure is calculated along the way that contains the highest number of high symmetry points of the Brillouin zone, F(1/2, 1/2, 0), Γ (0, 0, 0), Z(1/2, 1/2, 1/2), L(0, 1/2, 0). It can be seen that CuGaO₂ is an indirect gap (F- Γ point) material with the gap of 1.101 eV. Our calculated band gap is in good agreement with other theoretical calculation values, which are reported to be 1.04 eV [22] and 1.10 eV [24]. By considering PDOS, it

is clearly seen that the conduction band minimum states are mainly dominated by Cu-3p⁶, O-2p⁴ and Ga-4s² states, whereas the valence band maximum states are mainly composed of hybridized Cu-3d¹⁰ and O-2p⁴ states.

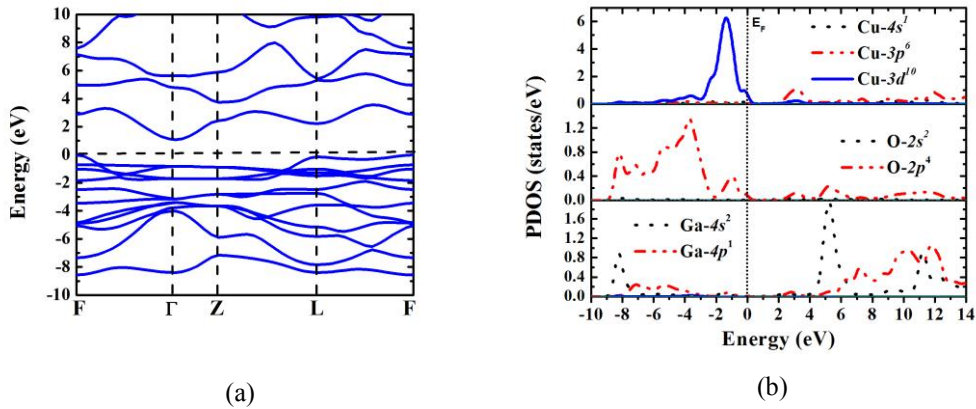


Fig. 2. (a) Calculated energy band structure; (b) calculated partial density of states, of CuGaO₂

According to rigid band approach, the effect of *p*-type acceptor doping level can be considered by varying the acceptor doping levels from 172 to 214 meV above the maximum valence band. Note that the Fermi energy is located at approximately 186 meV by comparing with the experimental Seebeck coefficient [19] and hole concentration [25]. From PDOS, the electronic structure can be reorganized by doping the impure atom at the *A* or *B* sites to study the effect of the acceptor doping levels. For example, the electrical conductivity significantly increased when the Pt was substituted in Cu_{1-x}Pt_xFeO₂ due to the increasing hole carrier [26]. The resistivity of the 5% Mg-doped delafossite CuCr_{1-x}Mg_xO₂ film rapidly decreased from 67 to 0.025 Ωcm [27]. The conductivity of CuY_{0.94}Ca_{0.06}O₂ is more than four orders of magnitude higher than that CuYO₂ at the room temperature [28]. The carrier concentrations of CuCrO₂ are increased by doping Mg in Cr atom site from 3.14 × 10¹⁵ cm⁻³ to 3.14 × 10¹⁸ cm⁻³ which is the main cause of the decrease of the resistivity [29]. These results indicated that the low (high) hole concentration can be obtained by shifting acceptor doping levels up (down).

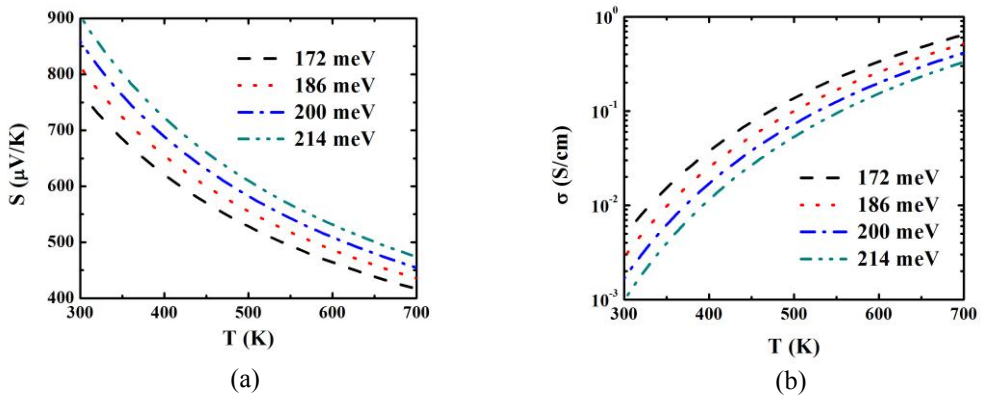


Fig. 3. Calculated transport coefficients: (a) Seebeck coefficient; (b) electrical conductivity as a function of absolute temperature for different acceptor doping levels

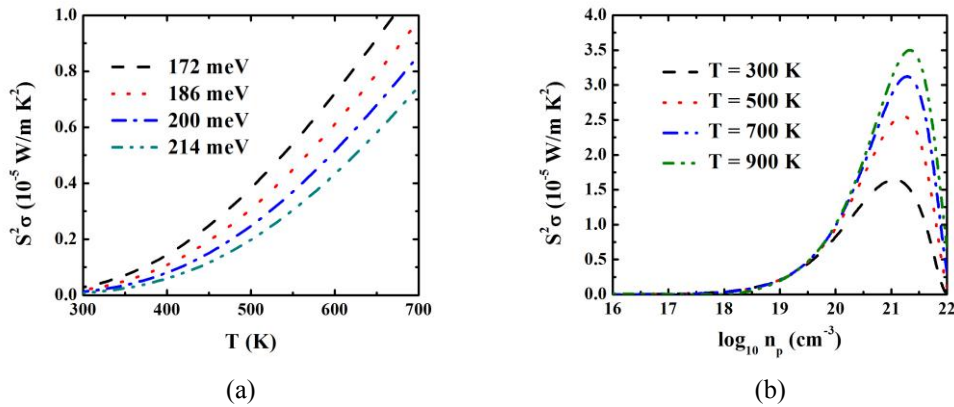


Fig. 4. Calculated power factor, $S^2\sigma$ as a function of: (a) absolute temperature; (b) hole concentration

The calculated temperature-dependent Seebeck coefficient for different acceptor doping levels is demonstrated in Fig. 3(a). It can be seen that Seebeck coefficient exponentially decreases with increasing temperature. This result is in agreement with experimental results reported by R.B. Gall et al. [20]. The electrical conductivity is also calculated as a function of temperature. Results are shown in Fig. 3(b). The increasing carrier concentration (the decreasing acceptor doping level) gives rise to the increase of the electrical conductivity as found in the common semiconductors [30]. The constant scattering time in Eq. (3) is obtained to be 0.4×10^{-16} s by fitting our calculated electrical conductivity respect to the constant scattering time with the experimental temperature-dependent electrical conductivity [20] at the Fermi energy. Fig. 4(a) shows the calculated PF in CuGaO_2 for various values of p -type acceptor doping levels. It can be seen that the PF increases with increasing temperature and p -type acceptor doping level. The trends of PF in the CuGaO_2 is similar to the trends of the other delafossite materials which is obtained by the experimental observations [26, 31–33]. The hole concentration dependence of PF are demonstrated in Fig. 4(b). It is indicated that the CuGaO_2 is a promising the TE material at metallic carrier density ($1 \times 10^{21} \text{ cm}^{-3}$ - $5 \times 10^{21} \text{ cm}^{-3}$) and high temperature.

4. Conclusion

In summary, the calculations based on density functional theory and Boltzmann transport theory were performed to investigate the electronic structures and TE properties for the delafossite p -type CuGaO_2 . The energy band structure shows the indirect band gap of CuGaO_2 with 1.101 eV and the Fermi energy is at 186 meV above the top valence band. The corresponding carrier concentration is $4.02 \times 10^{17} \text{ cm}^{-3}$. The average scattering time is 0.4×10^{-16} s. By considering the effects of p -type doping and temperature on TE properties, it is found that the PF increases with increasing acceptor doping level and temperature. It is concluded that the delafossite material CuGaO_2 can be considered as a promising TE material at high temperature and high p -type doping.

Acknowledgements

P.P. acknowledges Ubon Ratchathani Rajabhat University and the Science Achievement Scholarship of Thailand (SAST).

References

- [1] Goldsmith JH, *Thermoelectric Refrigeration*. New York: Plenum; 964.
- [2] Ohtaki M, Araki K, Yamamoto K. High thermoelectric performance of dually doped ZnO ceramics. *J Electron Mater* 2009;**38**:1234-8.
- [3] Poudel B, et al. High-thermoelectric performance of nanostructured bismuth telluride bulk alloys. *Science* 2008;**320**:634-8.
- [4] Banerjee AN, Maity R, Ghosh PK, Chattopadhyay KK. Thermoelectric properties and electrical characteristics of sputter-deposited p-CuAlO₂ thin films. *Thin Solid Films* 2005;**474**:261-6.
- [5] Prewitt CT, Shannon RD, Rogers DB. Chemistry of noble metal oxides. II. crystal structures of PtCoO₂, PdCoO₂, and AgFeO₂. *Inorg Chem* 1971;**10**:719-23.
- [6] Park K, Ko KY, Seo W-S. Thermoelectric properties of CuAlO₂. *J Eur Ceram Soc* 2005;**25**:2219-22.
- [7] Kim DS, Park SJ, Jeong EK, Lee HK, Choi SY. Optical and electrical properties of p-type transparent conducting CuAlO₂ thin film. *Thin Solid Films* 2007;**515**:5103-8.
- [8] Gurunathan K, Baeg JO, Lee SM, Subramanian E, Moon SJ, Kong KJ. Visible light assisted highly efficient hydrogen production from H₂S decomposition by CuGaO₂ and CuGa_{1-x}In_xO₂ delafossite oxide bearing nanostructured Co-catalysts. *Catalysis Commun* 2008;**9**:395-402.
- [9] Marquardt MA, Ashmore NA, Cann DP. Crystal chemistry and electrical properties of the delafossite structure. *Thin Solid Films* 2006;**496**:146-56.
- [10] Huda MN, Yan Y, Walsh A, Wei SH, Al-Jassim MM. Group-IIIA versus IIIB delafossites: electric structure study. *Phys Rev B* 2009;**80**:035205-1-7.
- [11] Liu Q-J, Liu Z-T, Feng L-P. Theoretical calculations of mechanical, electronic, chemical bonding and optical properties of delafossite CuAlO₂. *Physica B* 2010;**405**:2028-33.
- [12] Poopanya P, Yangthaisong A, Rattanapun C, Wichianchai A. Theoretical study of electronic structure and thermoelectric properties of doped CuAlO₂. *J Electron Mater* 2011;**40**:987-91.
- [13] Singh DJ. Band structure and thermopower of doped YCuO₂. *Phys Rev B* 2008;**77**:205126-1-5.
- [14] Zhang L, Singh DJ. Electronic structure and thermoelectric properties of layered PbSe-WSe₂ materials. *Phys Rev B* 2009;**80**:075117-1-8.
- [15] G.K.H. Madsen. Automated search for new thermoelectric materials: The case of LiZnSb. *J Am Chem Soc* 2006;**128**:12140-6.
- [16] Li J, Sleight AW, Jones CY, Toby BH. Trends in negative thermal expansion behavior for AMO₂ (A = Cu or Ag; M = Al, Sc, In, or La) compounds with the delafossite structure. *J Solid State Chem* 2005;**178**:285-94.
- [17] Clark SJ, et al. First principles methods using CASTEP. *Z Kristallogr* 2005;**220**:567-70.
- [18] Madsen, GKH, Singh DJ. BoltzTraP. A code for calculating band-structure dependent quantities. *Comput Phys Commun* 2006;**175**:67-71.
- [19] Gall RB, Ashmore N, Marquardt MA, Tan X, Cann DP. Synthesis, microstructure, and electrical properties of the delafossite compound CuGaO₂. *J Alloy Compd* 2005;**391**:262-6.
- [20] Kumekawa Y, et al. Evaluation of Thermodynamic and Kinetic Stability of CuAlO₂ and CuGaO₂. *J Therm Anal Calorim* 2010;**99**:57-63.
- [21] Ataoui KE, et al. Delafossite oxides containing vanadium(III): preparation and magnetic properties. *Solid State Sci* 2005;**7**:710-7.
- [22] Zhi-Jie F, Cheng F, Li-Jie S, Yong-Hui L, Man-Chao H. First-principles study of defects in CuGaO₂. *Chin Phys Lett* 2008;**25**:2997-3000.
- [23] Jayalakshmi V, Murugan R, Palanivel B. Electronic and structural properties of CuMO₂ (M = Al, Ga, In). *J Alloy Compd* 2005;**38**:19-22.
- [24] Robertson J, Xiong K, Clark SJ. Band gaps and defect levels in functional oxides. *Thin Solid Films* 2006;**496**:1-7.
- [25] Varadarajan V, Norton DP. CuGaO₂ thin film synthesis using hydrogen-assisted pulsed laser deposition. *Appl Phys A* 2006;**85**:117-20.
- [26] Ruttanapun C, et al. Thermoelectric properties of Cu_{1-x}Pt_xFeO₂ (0.0 ≤ x ≤ 0.05) delafossite-type transition oxide. *J Alloy Compd* 2011;**509**:4588-94.
- [27] Li D, et al. Characteristics of CuCr_{1-x}Mg_xO₂ films prepared by pulsed laser deposition. *J Alloy Compd* 2009;**486**:462-7.
- [28] Deng Z, et al. Effect of Ca-doping on the structural and electrical properties of CuY_{1-x}Ca_xO₂ (0 ≤ x ≤ 0.10) ceramics. *J Alloy Compd* 2011;**509**:5300-4.
- [29] Wang Y, Gu Y, Wang T, Shi W. Structural, optical and electrical properties of Mg-doped CuCrO₂ thin films by sol-gel processing. *J Alloy Compd* 2001;**509**:5897-902.
- [30] Boer KW. *Survey of Semiconductor Physics*. Van Nostrand Reinhold, 1990.
- [31] Park K, Ko KY, Kwon H-C, Nahm S. Improvement in thermoelectric properties of CuAlO₂ by adding Fe₂O₃. *J Alloy Compd* 2007;**437**:1-6.
- [32] Hayashi K, Nozaki T, Kajitani T. Structure and high temperature thermoelectric properties of delafossite-type oxide CuFe_{1-x}Ni_xO₂ (0 ≤ x ≤ 0.05). *Jpn J Appl Phys* 2007;**46**:5226-9.
- [33] Yanagiya S-i, Nong NV, Xu J, Pryds N. The effect of (Ag, Ni, Zn)-addition on the thermoelectric properties of copper aluminate. *Materials* 2010;**3**:318-28.